

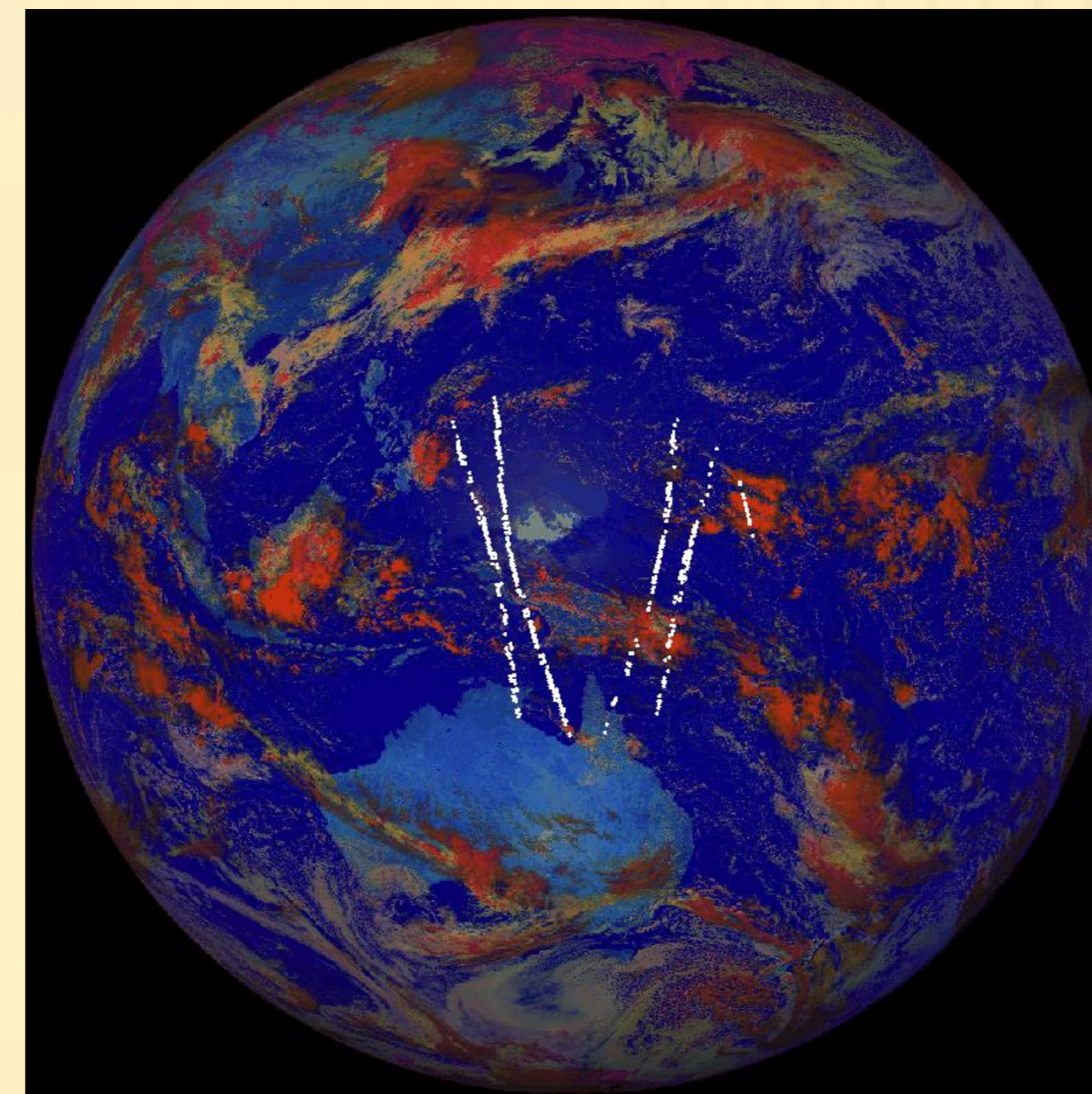
Characterization of AHI IR Channels with IASI measurements

Bertrand Théodore, Dorothee Coppens, Dieter Klaes

EUMETSAT, Eumetsat-Allee 1, 64295 Darmstadt, Germany

Introduction

Japan's next generation geostationary meteorological satellite "Himawari" has been successfully launched in October 2014 and placed over the West-Pacific. It carries the Advanced Himawari Imager (AHI) that provides images of the Earth in 16 bands in the visible and infrared domains every 10 minutes. As part of the operational monitoring of the products measured from the Infrared Atmospheric Sounding Interferometer (IASI) instruments currently flying on Metop-A and B, EUMETSAT has initiated a comparison of the infrared channels of AHI with collocated IASI measurements. Since the launch of the first IASI in 2007, the instrument has proven an excellent reference for inter-calibration studies thanks to a well characterized calibration, a very good stability in time and a continuous spectral coverage from 3.6 to 15.5 microns.



Collocations

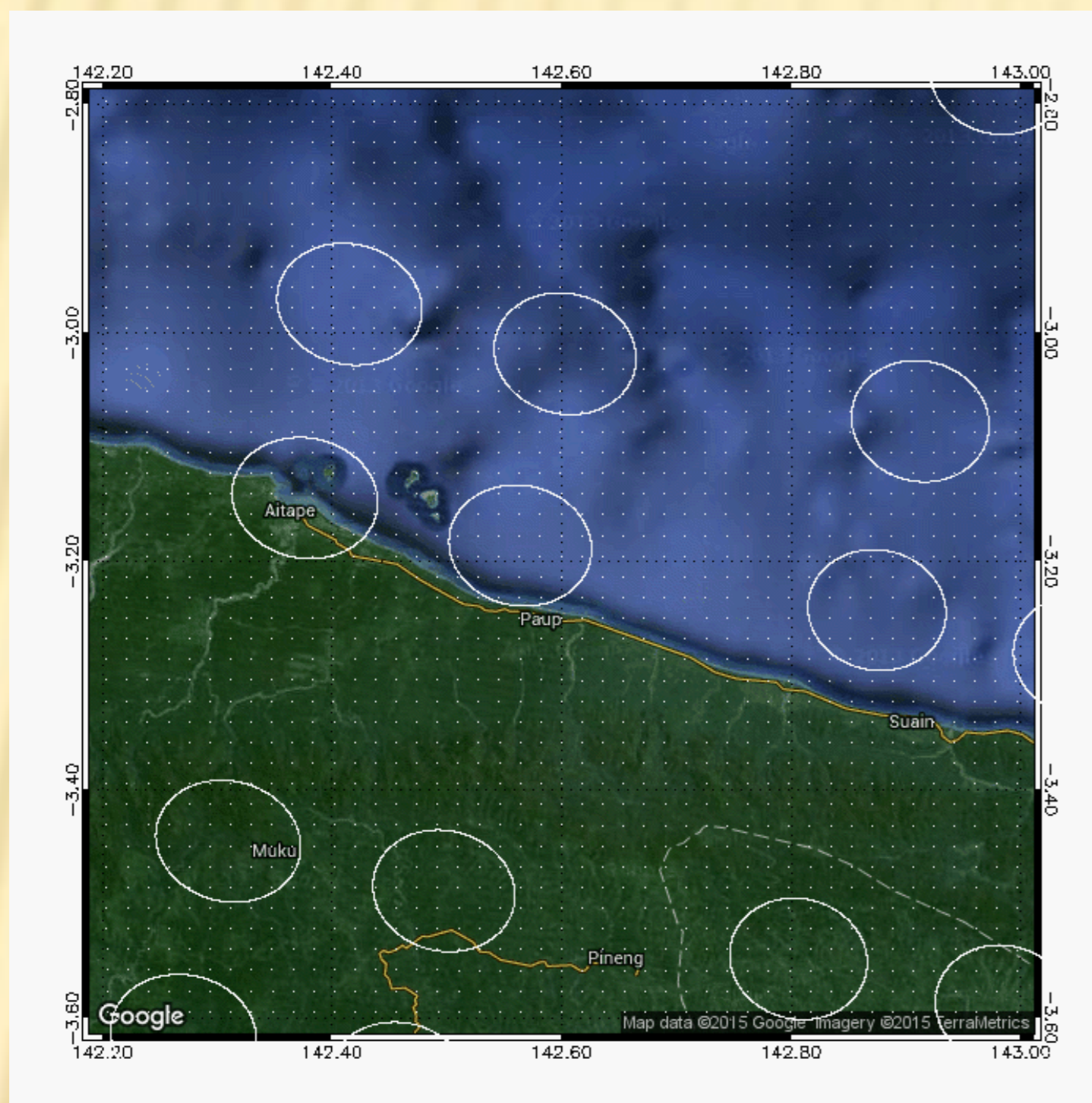
We have adopted the collocation criteria from the Global Space-based Inter-Calibration System (GSICS):

- * Time difference between observations less than the AHI repeat cycle (10 minutes)
- * Surface incidence angle from IASI less than 15 degrees from zenith
- * Difference between the surface incidence angles of the two instrument less than 2 degrees

The locations of the IASI-AHI data that meet these criteria on one day are shown here as white dots.

Spatial averaging

To ensure that both instruments have comparable spatial scales, the AHI pixels (delineated by white crosses) within the nominal area of each IASI field of view (represented here as white ellipses) are averaged and the variance of these pixels' radiance is used to estimate the spatial variability.

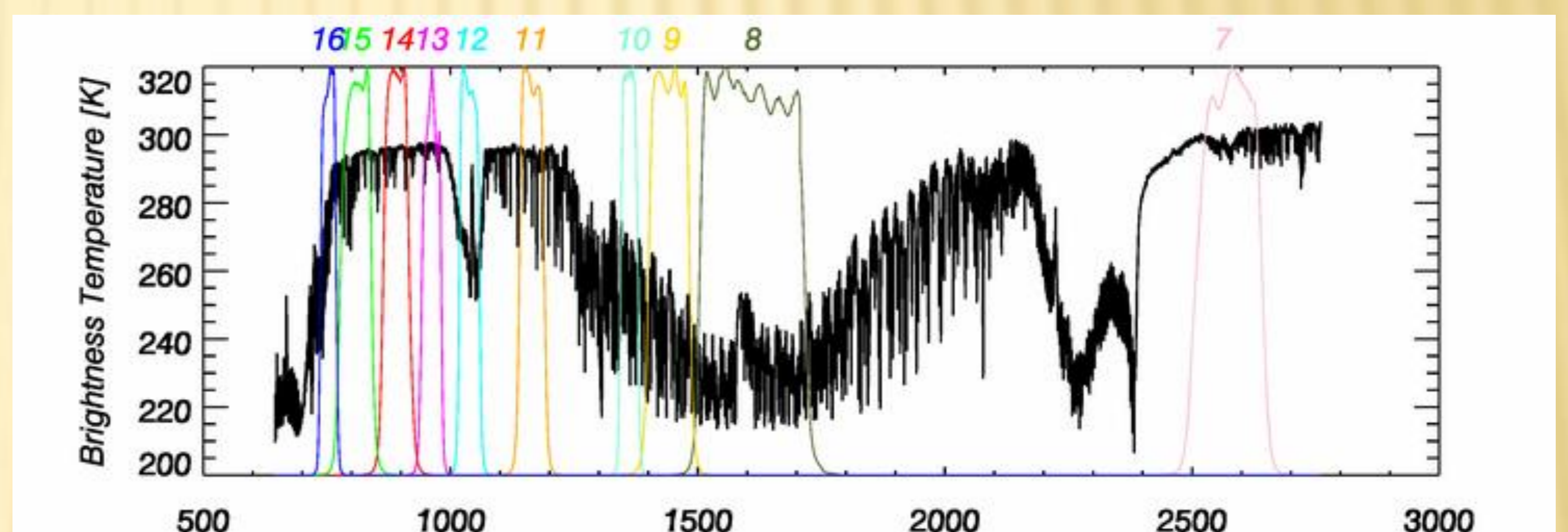


Spectral convolution

The radiance spectrum measured by IASI in each pixel is convolved with the Spectral Response Function (SRF) of each AHI channel interpolated on the IASI spectral resolution to allow direct comparison of their radiances:

$$L_j = \frac{\int SRF_j(\nu)L(\nu)d\nu}{\int SRF_j(\nu)d\nu}$$

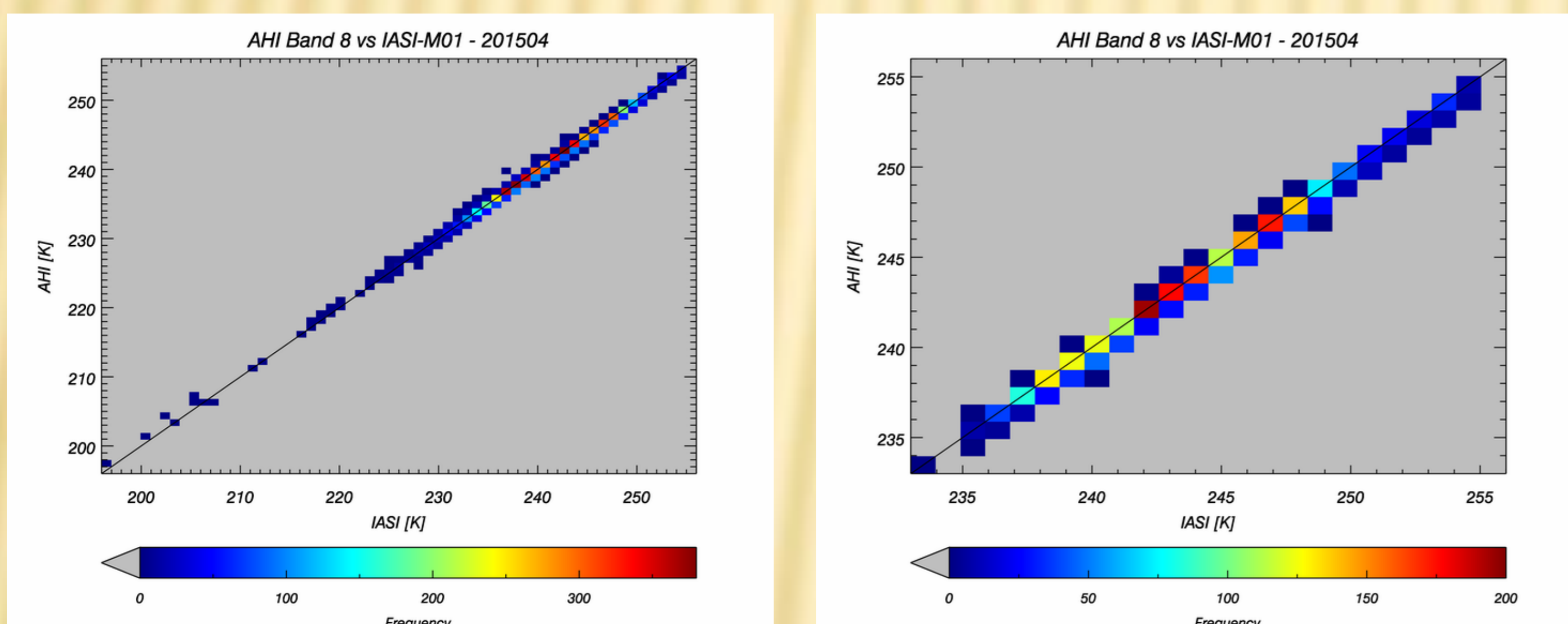
The spectral position of AHI SRFs is shown here on a typical clear-sky IASI spectrum



Results

Scatter plots

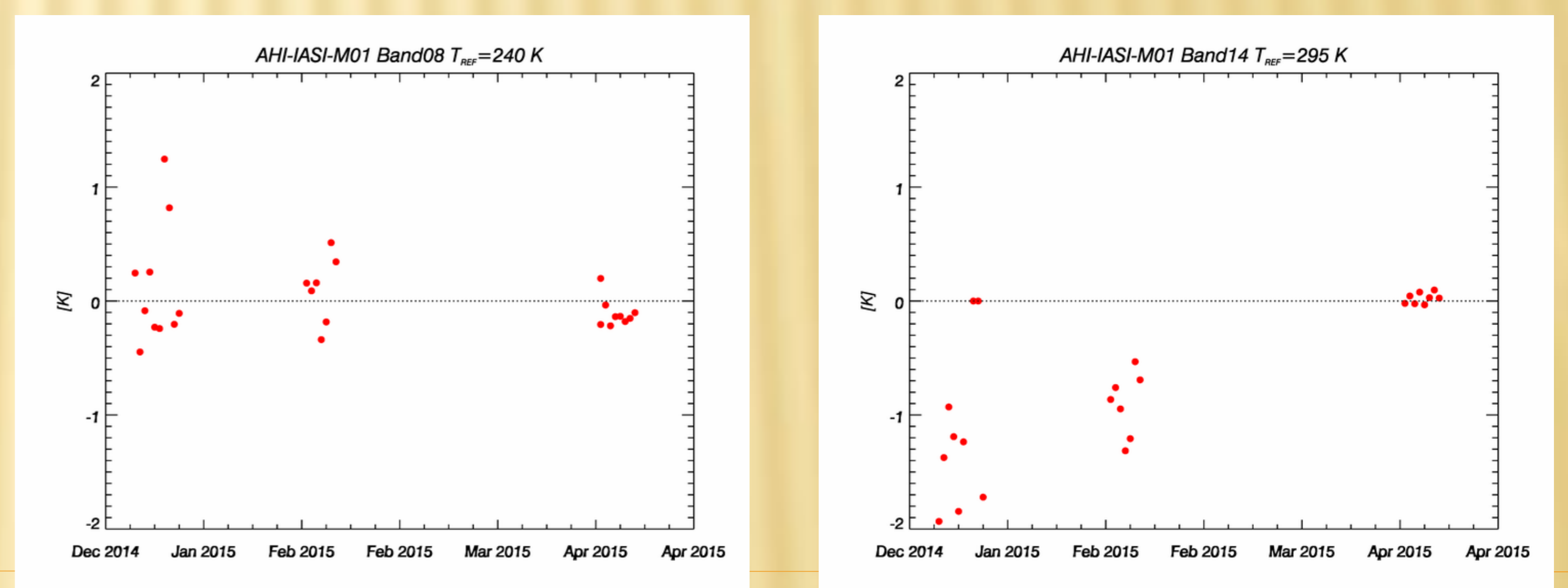
All collocations for which the estimated spatial variability of the AHI radiances is lower than 5% have been retained for the comparison. That includes possibly homogeneous cloud-covered pixels.



The agreement between IASI and AHI is excellent for instance in band 8, as plotted here for April 2015, with almost no dependency with the scene temperature, whether all homogeneous collocations are included (left plot) or with only IASI FoVs that are flagged as clear (right plot).

Time evolution

Because the slope of the regression is not necessarily equal to 1, the bias between both instruments may depend on the scene temperature. In order to facilitate the comparisons, we have defined a reference radiance (resp. temperature) for each channel that is typical for a clear sky scene over sea in this region. The bias between both instruments for this reference temperature can thus be computed for each day and plotted as a function of time for each band.



Three AHI datasets were available: January, February and April 2015. The improvement over time as the AHI commissioning is progressing is particularly visible: the bias between AHI and IASI has clearly decreased, along with its variance, to reach near-zero values.

Conclusion

Using the framework developed for the GSICS to perform an inter-comparison between IASI and AHI, we have found that the difference between AHI and IASI in clear sky have largely been reduced in all bands as AHI was commissioned. The biases are, as of April 2015, still slightly negative and of the order of -0.1 K in all bands.

Band	8	9	10	11	12	13	14	15	16
Tref	244	254	264	293	275	295	295	290	277
AHI-IASI (K)	-0.14	-0.19	0.00	-0.09	-0.26	-0.05	0.05	-0.06	0.07